

Measurement of thermal conductivity of thin films with a Si-N membrane-based microcalorimeter

B. L. Zink,^{a)} B. Revaz,^{b)} J. J. Cherry, and F. Hellman^{c)}

Department of Physics, University of California, San Diego, La Jolla, California 92093

(Received 24 September 2002; accepted 15 November 2004; published online 6 January 2005)

We describe a method of measuring thermal conductivity of films as thin as 15 nm from 2–300 K and in magnetic fields up to at least 8 T using a silicon-nitride membrane based microcalorimeter. The thermal transport in the membrane is measured before and after a sample film is deposited on the membrane. Accurate knowledge of the geometry of the microcalorimeter allows the thermal conductivity of the sample film to be determined from the difference of these measurements. We demonstrate the method for two thin film samples, a 16 nm thick Au film and a 200 nm Pb film. Results are in good agreement with the expected thermal conductivity. Below 10 K, surface scattering effects in the nitride membrane become important and limit the usefulness of this technique in some cases. Above 100 K radiative loss becomes important; we describe a method for correcting for this, taking advantage of its temperature dependence. © 2005 American Institute of Physics. [DOI: 10.1063/1.1848658]

I. INTRODUCTION

The thermal conductivity k of thin film materials is an important quantity for both industrial applications and fundamental science which has historically been difficult to measure. Thin films are the major constituent in many modern technologies where heat flow is critical. For metals, thermal engineering of integrated circuits and other micromachined devices usually relies on estimates of k calculated using the Wiedemann-Franz law $k/\sigma=L_oT$, where σ is the electrical conductivity and $L_o=2.44\times 10^{-8}$ W- Ω/K^2 is a constant commonly called the Lorenz number. Measurements of k as a function of T allow investigation of deviations from this behavior, which is not only of practical importance but also provides information about electron-phonon scattering and the contribution of phonons to thermal conductivity. For insulating thin films, the Wiedemann-Franz law does not apply, and values of k must be measured. Bulk values of k are often used, if they are known, though many insulating materials either cannot be made in bulk form or have not been thermally characterized. In addition, k often depends on microstructure and preparation technique, making the use of bulk values for thin films questionable. Several methods for measuring k for films of various thicknesses have been reported.^{1–11} These techniques are all either limited in temperature range, measure thicker films, or ignore effects of radiation.

In this article we describe a technique for measuring k of films between 10 and 200 nm thick, at temperatures from 2–300 K and in magnetic fields as large as 8 T. The measure-

ment is made using a Si-N membrane microcalorimeter and is useful for metallic, insulating or superconducting thin films. We present measurements of a 200 nm Pb film and a 16 nm Au film in addition to the bare microcalorimeter which is dominated by k of Si-N. Above 100 K radiation contributions become significant; we present means to determine this radiation loss. Below 10 K surface phonon scattering is important; we discuss results for membranes with different surface properties to demonstrate these effects. We also discuss the expected uncertainty and the range of thin films which can be effectively measured.

II. PRINCIPLE OF MEASUREMENT

The microcalorimeter, originally used to measure the heat capacity of thin films and described in detail elsewhere,^{12,13} requires no modification for thermal conductivity measurements. It consists of a 1 cm \times 1 cm single crystal silicon frame which supports a 200 nm thick, 0.5 cm \times 0.5 cm square low-stress amorphous Si-N membrane which is grown by low-pressure chemical vapor deposition (LPCVD) at ≈ 835 °C. Thin-film Pt heaters and Pt and amorphous niobium-silicon thermometers are vapor deposited and lithographically patterned on the central 0.25 cm \times 0.25 cm square area of the membrane. The top-view schematic inset in Fig. 1 indicates the location of the Pt heater and the thermometers. The microcalorimeters used for this study incorporate a SiO₂ layer between the Si wafer and the Si-N film to lower the stray capacitance between the Pt leads and heater and ground. This layer is either an ≈ 1.5 μ m LPCVD SiO₂ film grown at ≈ 350 °C (commonly referred to as low-temperature oxide, LTO) or an ≈ 600 nm thermal oxide layer, which is grown by oxidizing the silicon surface at 1000 °C. The thick LTO film often forms with voids and some thickness variation, while the thermal oxide is typically of higher quality, with less variation in thickness. The oxide

^{a)}Current address: National Institute of Standards and Technology, 325 Broadway MC 817.03, Boulder, CO 80305; electronic mail: bzink@boulder.nist.gov

^{b)}Current address: University of Geneva, Dept. of Condensed Matter Phys., CH-1211 Geneva 4, Switzerland.

^{c)}Current address: Dept. of Physics, UC Berkeley, CA 94720-7300.

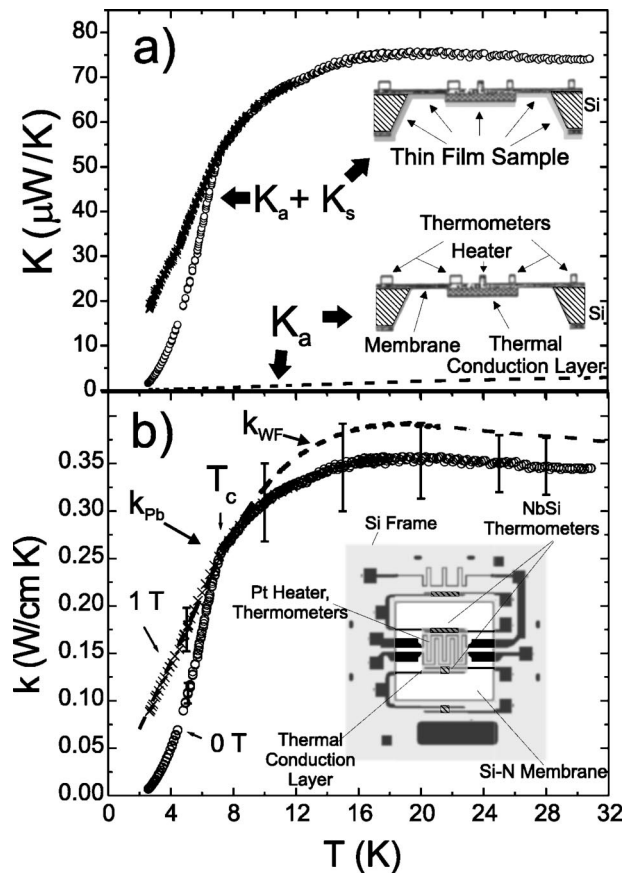


FIG. 1. (a) K_{meas} with the 200 nm Pb film deposited. K_s of this rather thick film is very large compared to K_a , which is barely visible above the temperature axis. Insets are side-view schematics of the calorimeter before and after sample deposition. (b) k_{Pb} in both superconducting (zero field) and normal (one tesla) states. Inset is a top view schematic of the calorimeter.

is removed from the membrane after it is formed by etching the Si wafer in KOH, but its presence during the growth of the Si-N affects the properties of the nitride surface on which samples are deposited.¹⁴ In order to keep the heater and thermometers isothermal, a 0.25 cm \times 0.25 cm thermal conduction layer (typically 200–400 nm of Ag, Au, Cu, or Al) is deposited on the back of the membrane through a micromachined shadow mask held within 25 μm of the membrane.

The Si-N membrane and Pt leads form a small thermal link from the central area of the membrane to the Si frame. We measure the conductance of this thermal link K_a by applying a small amount of heating power P by causing a known current to flow in the heater. When thermal equilibrium is reached, the thermal conduction layer, heater, and thermometers are at $T_o + \Delta T$, while the silicon frame remains at T_o . At this point the change in the resistance of the thermometer, $\Delta R = R(T_o + \Delta T) - R(T_o)$, is measured. ΔR is converted to temperature and ΔT determined using a calibration of the thermometer obtained by measuring R at each temperature T_o .

Below 100 K the heating power is related to the steady-state ΔT by $P = \langle K_a(T, T_o) \rangle \Delta T$. Here $\langle K_a(T, T_o) \rangle$ is the average thermal conductance of the link over the temperature range $(T_o, T_o + \Delta T)$. $K_a(T)$ is determined from this average with a two-variable fit. In practice we find that K_a is close to linear over the small values of ΔT (typically 1–10 % of T_o)

and we replace the average $\langle K_a(T, T_o) \rangle \cong K_a(T_o + \Delta T/2)$, giving the thermal conductance as a function of a single temperature.

K_a has contributions from the Pt leads, K_{Pt} , and the Si-N membrane, $K_{\text{Si-N}}$. To measure k we deposit the sample film on the entire back of the membrane. This adds another contribution, K_s to the thermal link so that $K_{\text{meas}} = K_{\text{Si-N}} + K_{\text{Pt}} + K_s = K_a + K_s$. K_s is then determined by subtracting K_a from the total thermal conductance after sample deposition, K_{meas} . Above 100 K, where radiation contributions become significant, and below 10 K, where surface scattering affects thermal transport in the membrane, K_s may not be determined by this simple subtraction. These more complicated cases are discussed below.

Once K_s is measured the sample's thermal conductivity k_s may be determined using the geometry of the microcalorimeter. Since the temperature gradient through the ≈ 200 nm thickness of the membrane is small compared to the gradients in the lateral dimensions of the microcalorimeter the system is essentially two-dimensional so that $k_s = K_s / \alpha t$, where α is a 2- d geometry factor and t is the sample film thickness. This assumption is good as long as thermal boundary resistances between the thin-film layers are negligible. When the central heater/thermometer area is isothermal, $\alpha = 10.33$.¹³ Simulations of the microcalorimeter presented elsewhere¹³ calculate deviation from this behavior when the thermal conductivity of the membrane/sample region is not \ll than that of the central area. The results set a limit on the technique as will be discussed below.

We have previously shown experimentally that applied magnetic fields have $< 1\%$ effect on K_a up to at least 8 T.¹⁵ Determining the field dependence of a film's k_s from a series of K_{meas} measurements in different steady-state applied fields therefore requires only one measurement of K_a in zero field. The niobium-silicon low temperature thermometers do show measurable magnetoresistance below 6 K,¹⁵ and must be calibrated for each measurement field at low T .

A. Surface scattering

As T drops, scattering of phonons is less frequent and the mean-free path increases. As the mean-free path approaches the thickness of the membrane, scattering of phonons from the membrane surface alters the thermal transport. If this scattering is specular the mean-free path continues to grow as temperature drops. When surface scattering is diffuse, the mean-free path and the thermal conductance are reduced. Measurements presented elsewhere suggest that below 10 K Si-N membranes grown on thermal oxide underlayers allow specular scattering while the scattering in membranes grown on LTO is predominantly diffuse.¹⁴

Several authors have reported that a change from specular to diffuse scattering can occur when particles or films are deposited on clean surfaces.^{11,16} When this occurs at the Si-N membrane surface, the contributions to the thermal conductance are not simply additive so that subtracting K_a from K_{meas} gives an artificially reduced value for K_s . We discuss the consequences of these surface scattering effects for low temperature measurements of k_s below.

B. Radiative contributions

For $T > 100$ K the radiation contributions are significant and become particularly important when the addition of the sample film changes the optical properties of the device. A first order estimate of the radiation correction begins by adding terms for the emission of radiation from the heated area of the calorimeter and absorption of radiation from the environment (kept at T_o by a radiation shield) so that

$$P = \langle K_{\text{cond}}(T, T_o) \rangle \Delta T + A_{\text{eff}} \epsilon \sigma [(T_o + \Delta T)^4 - T_o^4], \quad (1)$$

where $\sigma = 5.67 \times 10^{-12}$ W/cm²K⁴ is the Stefan-Boltzmann constant, A_{eff} and ϵ are the effective area and emissivity of the heated surfaces, and $K_{\text{cond}} = K_{\text{Si-N}} + K_{\text{Pt}}$ is the non-radiative contribution. Using a Taylor expansion for K_{cond} and taking terms up to ΔT gives $P/\Delta T \cong K_{\text{cond}}(T_o) + 4A_{\text{eff}}\epsilon\sigma T_o^3$, indicating that radiation adds a T^3 term to the quantity measured at low T . One method for removing the radiation term is to assume that at high T K_{cond} does not contain T^3 terms. We fit $P/\Delta T = K$ above 100 K to $K = a_0 + a_1T + a_2T^3$, calculate $A_{\text{eff}}\epsilon = a_2/4\sigma$ and subtract $4A_{\text{eff}}\epsilon\sigma T_o^3$ from K at all T . This method is relatively simple and effective as long as ΔT is small and K_{Pt} and $K_{\text{Si-N}}$ do not contain T^3 terms above 100 K.

Though calculating $A_{\text{eff}}\epsilon$ is sufficient to remove radiation losses and determine K_{cond} , determining ϵ requires some knowledge of A_{eff} . This is complicated due to the different optical properties of different elements of the nonuniformly heated membrane. We can make a simple estimate of A_{eff} by assuming that ϵ of the Si-N surfaces is $\gg \epsilon$ of the metal surface of the conduction layer, ignoring the relatively small surface area of the Pt leads and heater and assuming the central area is isothermal at $T_o + \Delta T$. In this case radiation is emitted from the top surface of the 0.25 cm \times 0.25 cm central area and the top and bottom surfaces of the membrane border which supports the temperature gradient. To further simplify we approximate the radiation from the border with radiation from a border isothermal at $T_o + \Delta T$ with an area scaled by the ratio of its average heating to ΔT .¹⁷ These approximations give $A_{\text{eff}} = 0.219$ cm².

A more general approach to correcting radiation loss where P is allowed to have ΔT^2 terms could be useful in some cases and is described elsewhere.¹⁸ Once the radiation contributions are determined both before and after sample film deposition, K_s is given by

$$K_s = [K_{\text{meas}} - 4\sigma\epsilon^* A_{\text{eff}}^* T_o^3] - [K_a - 4\sigma\epsilon A_{\text{eff}} T_o^3], \quad (2)$$

where $\epsilon^* A_{\text{eff}}^* = a_2/4\sigma$ are the values after deposition of the sample film which can significantly alter the emissivity of the bottom surface of the membrane.

III. EXPERIMENT

We first thermally evaporated a 300 nm Cu conduction layer on the central area of several microcalorimeters from the same wafer. We then thermally evaporated two sample films, a 200 nm thick Pb film (with a thin Ge underlayer which promotes growth of a flatter, continuous Pb film) and a 16.3 nm thick Au film, at base pressures of 4×10^{-6} Torr or lower simultaneously onto the microcalorimeters and several

Si-N coated Si substrates which were used for profilometry, electrical resistivity, and x-ray diffraction measurements. The thickness of the Pb/Ge layer was measured by profilometry after depositing a 20 nm thick Ag film to prevent the profilometer stylus from dragging through the soft Pb. The Pb film's x-ray diffraction pattern is typical of a (111)-textured polycrystalline fcc film with average crystallite size ≈ 56 nm. The electrical resistivity ρ of the Pb/Ge film was measured using a standard four lead technique using a 3 mm \times 1 cm strip broken from a larger substrate. Results are as expected for a bulk polycrystalline Pb film, T_c is 7.2 K and ρ approaches the impurity-dominated regime just above T_c with $\rho_o \approx 0.7$ $\mu\Omega$ -cm and residual resistivity ratio ≈ 27 , indicating a reasonably pure film.

The thickness of the Au film was determined by low-angle x-ray reflectometry and the ρ measured with a four lead technique on a photolithographically patterned film. It is important to note that 16.3 nm is an average thickness determined from interference fringes in the low-angle x-ray scan, and that the roughness of this film is likely of the same order of magnitude as the thickness. As is often the case in such thin metal films,¹⁹ ρ is dominated by transport through the thinner areas of the film, causing high residual resistivity, $\rho_o = 7.32$ $\mu\Omega$ -cm (ρ reaches ρ_o at ≈ 15 K), and $\partial\rho/\partial T$ approximately $2 \times$ higher than for bulk Au.

The microcalorimeter is cooled in a sample-in-vacuum ⁴He cryostat which is operated either in a storage dewar or in the bore of a superconducting magnet. The temperature of the sample stage, to which the microcalorimeter is attached with grease and a clamp, is monitored with a calibrated Lakeshore Cernox sensor and measurements of the microcalorimeter's thermometers are made with a lock-in amplifier and an ac resistance bridge described in detail elsewhere.¹²

IV. RESULTS AND DISCUSSION

Figure 1(a) shows K_{meas} from 2–30 K after deposition of the 200 nm thick Pb film. K_a is also shown in this temperature range, though $K_{\text{meas}} > 10 \times K_a$. Data in the normal state is obtained by applying a one tesla magnetic field which is well above H_c for Pb. Figure 1(b) shows thermal conductivity for the Pb film, k_{pb} versus T . The error bars on k are discussed below. As expected k_{pb} is exponentially suppressed in the superconducting state, and roughly linear in the normal state. A linear fit to the normal state data below T_c gives an estimate of the electron mean free path, $\ell = 3k/\gamma T v_F \approx 37.5$ nm, where v_F is the Fermi velocity and γ the density of electron states for Pb. ℓ is comparable to the estimate of the crystallite size 56 nm, determined from the x-ray line-width. The dashed line shows the prediction of the Wiedemann-Franz law, $k_{\text{WF}} = LT/\rho$, where ρ is the measured electrical resistivity of the Pb film. k_{WF} in the normal state was calculated assuming $\rho = \rho_o$ below T_c . The uncertainty on k_{WF} is $\sim 9\%$ and is dominated by the uncertainty of the geometry of the resistivity sample. The curves are within error bars from 2 to 30 K.

Figure 2(a) shows K_{meas} from 2–300 K after deposition of the 16.3 nm Au film. Again K_a is shown. Here K_a is $\approx 40\%$ of K_{meas} at high T and $\approx 70\%$ at low T . Note the

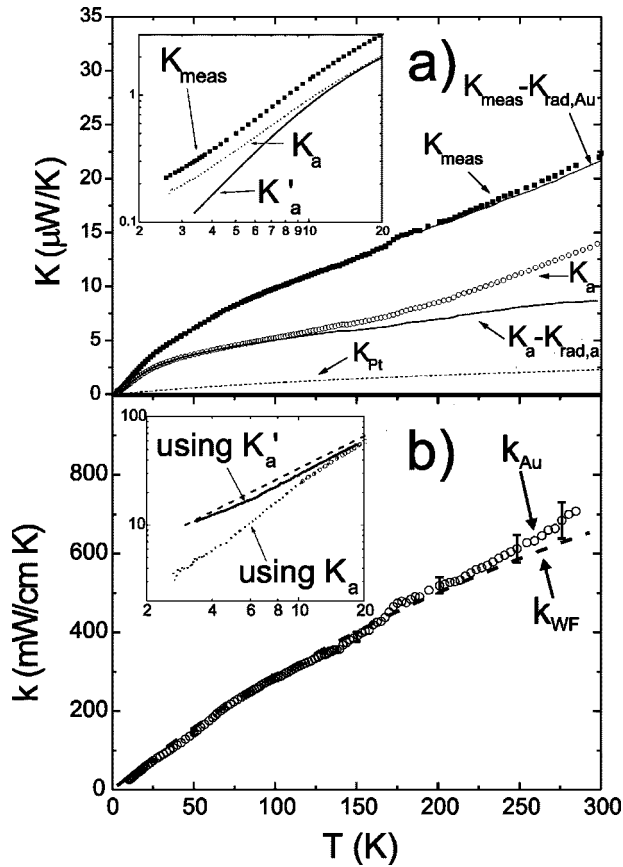


FIG. 2. (a) K_a vs T shown with K_{meas} after deposition of the thin Au film. Subtracting the radiation terms $K_{\text{rad},a} = 4\sigma\epsilon A_{\text{eff}} T_o^3$ and $K_{\text{rad},\text{Au}} = 4\sigma\epsilon^* A_{\text{eff}}^* T_o^3$ gives K_{cond} , shown with solid lines. K_{Pt} is shown by a dotted line. Inset: a low T log-log plot shows the effects of surface scattering. K_a is measured for the membrane grown on thermal oxide, while K'_a is measured for a membrane grown on LTO which is dominated by diffuse scattering. (b) k_{Au} vs T from 10–300 K. The dashed line is the prediction of the Wiedemann-Franz law. k_{Au} is $\approx 4\times$ lower than k_{bulk} at 300 K and shows roughly linear dependence for $T > 15$ K. Inset: k_{Au} obtained using K_a and K'_a .

upturn of K_a above ≈ 150 K which is the signature of the radiation term with its T^3 dependence, as well as the much smaller upturn in K_{meas} . The estimated emissivity for K_a is $\epsilon \approx 0.04 \pm 0.006$ (using $A_{\text{eff}} = 0.219 \text{ cm}^2$). After deposition of the Au sample the radiation contribution is much smaller; $\epsilon^* A_{\text{eff}}^* \approx \epsilon A_{\text{eff}}/8$. Radiation-corrected values appear in Fig. 2(a) as solid lines. K_{Pt} , calculated from the Wiedemann-Franz law using the measured ρ of the platinum heater, is shown as a dashed line. Subtraction of the radiation term and K_{Pt} from K_a gives $K_{\text{Si-N}}$ and $k_{\text{Si-N}}$. The results presented in another publication¹⁴ are similar to k of many glassy solids and agree well with other published values for a -Si-N films.

The inset of Fig. 2(a) is a low- T log-log plot of K_{meas} and K_a which shows the effect of surface scattering. The dotted line labeled K_a is the data measured on this microcalorimeter before deposition of the Au sample film. This membrane was deposited on a thermal oxide underlayer, causing specular scattering of phonons as described above. After deposition of the Au film, the surface scattering is at least partly diffuse,^{11,16} reducing the contribution of the membrane from the value measured with no sample. As a result $K_s \neq K_{\text{meas}} - K_a$, with this subtraction giving a potentially large underestimation of the contribution of the sample. The solid line

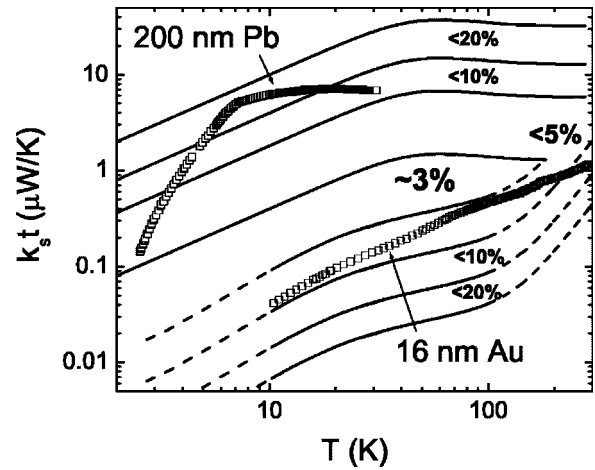


FIG. 3. Plot of the product of sample film thickness and sample thermal conductivity, $k_s t$, vs T . Solid contour lines show required values for estimated relative error on k_s to be 0.03, 0.05, 0.10, and 0.20. Dashed lines indicate conditions where estimate of error depends on details of the microcalorimeter or sample due to surface scattering (low T , low $k_s t$) or sample emissivity ($T > 100$ K). Symbols indicate measured values for the Pb and Au films.

labeled K'_a is the thermal conductance determined using $K_{\text{Si-N}}$ from a membrane grown on an LTO underlayer, where surface scattering is predominately diffuse. Subtracting K'_a provides an estimate of the true contribution of the sample film.

Figure 2(b) is a plot of the thermal conductivity of the Au film k_{Au} . Bulk Au typically has a constant $k \approx 3 \text{ W/cmK}$ from ≈ 80 –300 K, and a peak below 20 K.²⁰ Our k_{Au} is $\approx 4\times$ lower than bulk values, almost certainly from the same geometric effects of film roughness which increase ρ_o and $\partial\rho/\partial T$. k_{Au} is also roughly linear above ~ 15 K, suggesting it is dominated by electrons, with a weakly temperature-dependent mean-free path. Here a linear fit gives $\ell = 3k/\gamma v_F T \approx 9.5 \text{ nm}$. This is roughly half the measured average thickness of the film, which is consistent with a geometrical origin of the suppressed k and ρ . The dashed line shows k_{WF} for the Au film. Here the photolithographically patterned resistivity sample gives smaller uncertainty in geometry and $\sim 5\%$ uncertainty in k_{WF} . The two curves are within error bars above 50 K, giving additional evidence that the film roughness has a similar effect on both k and ρ . The slight reduction in k with respect to k_{WF} is consistent with the suppression of k with respect to σ often seen in metals below Θ_D (165 K for bulk Au). The inset in Fig. 2(b) shows k_{Au} at low T on a log-log plot. The result obtained using the specular scattering-dominated K_a appears as a dotted line. The solid line is the estimate of k_{Au} obtained by subtracting K'_a which is dominated by diffuse scattering as described above, and the dashed line is the prediction of the Wiedemann-Franz law. The diffuse-scattering estimation shows much better agreement with the Wiedemann-Franz law, supporting our interpretation of the surface scattering effects.

Figure 3 is a plot of the product of sample film thermal conductivity and film thickness, $k_s t$ versus T . The contour lines on this plot are calculated values of $k_s t$ required for the error on k_s to be 3%, 5%, 10%, and 20%. The dashed lines shown above 100 K and below 10 K are the radiation and surface scattering regions where the estimation of error de-

depends on sample emissivity and surface properties of both the sample and the nitride membrane. Below 100 K the lower $k_s t$ contour lines are set by the 1% uncertainty in measurement of K_a , and K_{meas} and the 2% uncertainty in t . Above 100 K the uncertainty in determining ϵ and ϵ^* (which depends on the optical properties of the sample film) is significant. Below 10 K the dashed lines are calculated assuming $K_s = K_{\text{meas}} - K_a$, which we expect for surface scattering that is predominantly diffuse. When measurements of K_a below 10 K are consistent with specular scattering, larger values of $k_s t$ are required ($\approx 0.1 \mu\text{W/K}$ or greater) to avoid large uncertainties due to surface scattering effects. The best way to eliminate surface scattering effects as a source of uncertainty is to measure a series of films of different thicknesses. K_s will scale with thickness if it is a meaningful measurement of film properties.

The upper $k_s t$ limits are set by the requirement for maintaining thermal equilibrium in the central heater and thermometer area. As described in detail elsewhere¹³, $\alpha = 10.33$ holds while the temperature gradient is confined to the area between the central conduction layer and the Si frame. As k_s or t for the sample film increases (relative to kt for the 300 nm Cu conduction layer), the temperature gradient across the conduction layer grows and α is reduced, leading to systematic underestimation of k_s which is calculated in Ref. 13.

Measured values of $k_s t$ for the Pb (superconducting state) and Au films are also plotted in Fig. 3. The two films span the range of thin films which can be measured with this technique. Figure 3 also suggests that our technique has good potential for measuring k for a range of metal films from 20 to 100 nm thick. To our knowledge no comprehensive study of $k(T)$ for such thin metal films exists, although evidence exists that the Wiedemann-Franz law is obeyed at least in limited cases.^{21,22} Films such as amorphous semiconductors typically have $k \sim 5 - 50 \times 10^{-4} \text{ W/cmK}$ at 5 K. Our method could measure 60–600 nm thick films in this range with uncertainty better than 5%.

ACKNOWLEDGMENTS

The authors would like to thank B. B. Maranville, R. Dynes, A. Frydman, O. Namaan, D. Cahill, B. Pohl, S.

Huxtable, and M. van der Burch for valuable discussions and other contributions, and the NSF (DMR 9705300 and DMR 0203907), UCDD at LANL, and the Swiss National Fund for Scientific Research for providing funding for this work.

¹D. G. Cahill, H. E. Fischer, T. Klitsner, E. T. Swartz, and R. O. Pohl, *J. Vac. Sci. Technol. A* **7**, 1259 (1989).

²D. G. Cahill, *Rev. Sci. Instrum.* **61**, 802 (1990).

³D. G. Cahill, W. K. Ford, K. E. Goodson, G. D. Mahan, A. Majumdar, H. J. Maris, R. Merlin, and S. R. Phillpot, *J. Appl. Phys.* **93**, 793 (2003).

⁴U. Bernini, S. Lettieri, P. Maddalena, R. Vitiello, and G. D. Francia, *J. Phys.: Condens. Matter* **13**, 1141 (2001).

⁵M. L. Grilli, D. Ristau, M. Dieckmann, and U. Willamowski, *Appl. Phys. A: Mater. Sci. Process.* **71**, 71 (2000).

⁶S. Moon, M. Hatano, M. Lee, and C. P. Grigoropoulos, *Int. J. Heat Mass Transfer* **45**, 2439 (2002).

⁷K. E. Goodson, M. I. Flik, L. T. Su, and D. A. Antoniadis, *IEEE Electron Device Lett.* **14**, 490 (1993).

⁸J. O. Willis and D. M. Ginsberg, *Phys. Rev. B* **14**, 1916 (1976).

⁹A. Irace and P. M. Sarro, *Sens. Actuators, A* **76**, 323 (1999).

¹⁰E. Jansen and E. Obermeier, *J. Micromech. Microeng.* **6**, 118 (1996).

¹¹W. Holmes, J. M. Gildemeister, P. L. Richards, and V. Kotsubo, *Appl. Phys. Lett.* **72**, 2250 (1998).

¹²D. W. Denlinger, E. N. Abarra, K. Allen, P. W. Rooney, M. T. Messer, S. K. Watson, and F. Hellman, *Rev. Sci. Instrum.* **65**, 946 (1994).

¹³B. Revaz, B. L. Zink, D. O'Neil, L. Hull, and F. Hellman, *Rev. Sci. Instrum.* **74**, 4389 (2003).

¹⁴B. L. Zink and F. Hellman, *Solid State Commun.* **129**, 199 (2004).

¹⁵B. L. Zink, B. Revaz, R. Sappey, and F. Hellman, *Rev. Sci. Instrum.* **73**, 1841 (2002).

¹⁶T. Klitsner, J. E. VanCleve, H. E. Fischer, and R. O. Pohl, *Phys. Rev. B* **38**, 7576 (1988).

¹⁷If we break the membrane border into equal squares, there are four corner squares at $\approx T_o + \Delta T/4$ and eight edge squares at $\approx T_o + \Delta T/2$. The scaled area of the border is then five squares, with both top and bottom surfaces giving 10 squares. The top surface of the isothermal central area adds four squares, so $A_{\text{eff}} = 14 \times 0.125 \text{ cm} \times 0.125 \text{ cm} = 0.219 \text{ cm}^2$. Note that this calculation only affects the determination of ϵ , not the product $A_{\text{eff}}\epsilon$, which is all that is required to subtract the radiation contribution from the measured thermal link.

¹⁸B. L. Zink, Ph. D. thesis, University of California, San Diego (2002).

¹⁹S. B. Arnason, S. P. Herschfield, and A. F. Hebard, *Phys. Rev. Lett.* **81**, 3936 (1998).

²⁰R. L. Powell and W. A. Blanpied, eds., *Thermal Conductivity of Metals and Alloys at Low Temperatures*, National Bureau of Standards Circular 556 (United States Department of Commerce, Washington, DC, 1954).

²¹R. T. Syme, M. J. Kelly, and M. Pepper, *J. Phys.: Condens. Matter* **1**, 3375 (1989).

²²T. Starz, U. Schmidt, and F. Volklein, *Sens. Mater.* **7**, 395 (1995).